This work is published in Phys. Rev. Lett. **93**, 256601 (2004).

Inelastic Scattering and Local Heating in Atomic Gold Wires

Thomas Frederiksen,[1,*] Mads Brandbyge,[1] Nicolás Lorente,[2] and Antti–Pekka Jauho[1]

[1] *MIC – Department of Micro and Nanotechnology, Technical University of Denmark, Ørsteds Plads, Bldg. 345E, DK-2800 Lyngby, Denmark*

[2] *Laboratorie Collisions, Agrégats, Réactivité, IRSAMC, Université Paul Sabatier, 118 Route de Narbonne, F-31062 Toulouse, France*

(Dated: February 2, 2008)

We present a method for including inelastic scattering in a first-principles density-functional computational scheme for molecular electronics. As an application, we study two geometries of four-atom gold wires corresponding to two different values of strain, and present results for nonlinear differential conductance vs device bias. Our theory is in quantitative agreement with experimental results, and explains the experimentally observed mode selectivity. We also identify the signatures of phonon heating.

PACS numbers: 72.10.Di, 73.23.-b, 73.40.Jn

Atomic-size conductors are the components of the emerging molecular electronics [1]. The corresponding molecular devices have new functionalities that exploit quantum phenomena, such as phase coherence and resonances. A substantial effort has been devoted to molecular electronics, producing a wealth of experimental data on electronic transport at the molecular level, e.g.,[2, 3, 4]. Most recently the issue of vibrational effects has drawn much attention since inelastic scattering and energy dissipation inside atomic-scale conductors are of paramount importance in device characteristics, working conditions, and – especially – stability [5, 6, 7].

Inelastic effects are interesting, not only because of their potentially detrimental influence on device functioning, but also because they can open up new possibilities and operating modes. Indeed, these effects have been used to identify the vibrational spectra of objects in tunneling junctions. This is the case of the inelastic electron tunneling spectroscopy (IETS) both in metal-insulator-metal junctions [8] and on surfaces with the scanning tunneling microscope (STM) [9]. Recently, similar vibrational signatures in the high-conductance regime have been revealed [3, 10, 11]. In one of these studies Agraït and co-workers used a cryogenic STM to create a free-standing atomic gold wire between the tip and the surface of the substrate. The STM was then used to measure the conductance against the displacement of the tip, making it possible to determine the approximate size as well as the level of strain of the wire. The data show distinct drops of conductance at particular tip-substrate voltages (symmetric around zero bias), consistent with the interpretation that the conducting electrons were backscattered from vibrations. It was assumed that that the onset of the drops coincided with a natural frequency of the wire at certain sizes and strains.

Several different theories have been put forward to address the effects of vibrations on electrical conductance. In the tunneling regime a substantial theoretical effort was undertaken right after the first experimental evidence [12] of vibrational signals in the tunneling conductance [13, 14]. Later, general tight-binding methods including inelastic effects were developed [15, 16]. More recently, the combination of *ab initio* techniques (such as the density-functional theory, DFT), and nonequilibrium Green's function (NEGF) techniques led to a microscopic understanding of conduction processes in the *elastic* regime, e.g., [17]. Detailed *ab initio* studies of IETS with STM have also appeared [18, 19]. To the best of our knowledge, only few realistic calculations have addressed inelastic effects in the high-conductance regime. Montgomery and co-workers [20, 21] used a lowest order perturbation theory (LOPT) approach for the electron-phonon (e-ph) interaction to estimate the inelastic contribution to the current through atomic gold wires within a tight-binding description. LOPT have also been combined with *ab initio* methods to study vibrational effects in point contacts and molecular junctions [22, 23]. LOPT cannot be applied in all circumstances; a point in case is polaronic effects which have been shown to be essential for the correct description of transport in long chains [24]. Unfortunately, going beyond LOPT is a highly nontrivial task; see, e.g., [25, 26, 27].

In this Letter we formulate a first-principles theory of electron transport including inelastic scattering due to phonons. We apply it to atomic gold wires, for which high quality experimental data are available, thus allowing a stringent test of the predictive power of our scheme. We employ DFT [28] for the electronic structure combined with an NEGF calculation of the steady current and power flow. We go beyond LOPT using the self-consistent Born approximation (SCBA) for the e-ph interaction. For gold wires we find that the only significant inelastic scattering mechanism is due to longitudinal modes with "alternating bond length" (ABL) character, and show how "heating" of these active modes can be identified in a transport measurement. The theoretically computed values for conductance changes, frequency shift with elongation, and slope in conductance

with voltage are in excellent agreement with experiments. The theory further shows that as the wire is stretched new vibrational modes become effective.

Our method consists of essentially three consecutive steps comprising the calculation of (i) mechanical normal modes and frequencies, (ii) electronic structure and e-ph couplings in a localized atomic-orbital (AO) basis set, and (iii) inelastic transport with NEGF. We partition the system into left (L) and right (R) electrode, and central device region (C), in such a way that the direct coupling between the electrodes is negligible. Hence we may write the electronic Hamiltonian as

$$\mathcal{H} = \mathcal{H}_L + \mathcal{V}_{LC} + \mathcal{H}_C(Q) + \mathcal{V}_{RC} + \mathcal{H}_R\,, \qquad (1)$$

where $\mathcal{H}_\alpha$ is a one-electron description of electrode $\alpha = L/R$ and $\mathcal{V}_{\alpha C}$ the coupling between α and C. The central part $\mathcal{H}_C(Q)$ depends explicitly on a $3N$-dimensional displacement variable Q which corresponds to mechanical degrees of freedom of N atoms in region C.

To obtain the most accurate normal modes Q_λ and frequencies Ω_λ within DFT of a given structure we employ a plane-wave (PW) basis [29]. Except for this purpose we use DFT with an nonorthogonal basis set of numerical AOs with finite range [17, 30, 31], which unambiguously allow us to partition the system as mentioned above. In this basis we expand the Q-dependence of the central part Hamiltonian to first order in Q_λ (since the vibrational amplitudes are small compared with the bond lengths), and write

$$\mathbf{H}_C(Q) \approx \mathbf{H}_C(0) + \sum_{\lambda=1}^{3N} \mathbf{M}^\lambda (b_\lambda^\dagger + b_\lambda), \qquad (2)$$

where $b_\lambda^\dagger$ (b_λ) is the creation (annihilation) operator of oscillator mode λ, and the coupling matrices $\mathbf{M}^\lambda$ are calculated using finite differences [32]. If the central region C is sufficiently large the coupling elements are localizable within its subset of the AO basis.

The transport calculation is based on NEGF techniques and the e-ph interaction treated within SCBA [26, 27, 33]. The electrical current I_α and the power transfer P_α *to* the device (per spin) from lead α are [26, 34]

$$I_\alpha = e\langle \dot{\mathcal{N}}_\alpha \rangle = \frac{-e}{\hbar}\int_{-\infty}^{\infty} \frac{d\omega}{2\pi} t_\alpha(\omega), \qquad (3)$$

$$P_\alpha = -\langle \dot{\mathcal{H}}_\alpha \rangle = \frac{1}{\hbar}\int_{-\infty}^{\infty} \frac{d\omega}{2\pi} \omega t_\alpha(\omega), \qquad (4)$$

$$t_\alpha(\omega) = \mathrm{Tr}[\mathbf{\Sigma}_\alpha^<(\omega)\mathbf{G}^>(\omega) - \mathbf{\Sigma}_\alpha^>(\omega)\mathbf{G}^<(\omega)], \qquad (5)$$

where $\mathcal{N}_\alpha$ is the electronic number operator of lead α, $\mathbf{G}^{\lessgtr}$ the electronic lesser/greater Green's function in the device region C, and $\mathbf{\Sigma}_\alpha^{\lessgtr}$ the lesser/greater self-energy due to coupling of C to α. We evaluate the SCBA e-ph self-energy $\mathbf{\Sigma}_{\rm ph}$ using free phonon Green's functions, which involve average mode occupations N_λ (also in nonequilibrium). The coupled equations for $\mathbf{G}$ and $\mathbf{\Sigma}_{\rm ph}$ are iterated until self-consistency is achieved. This approximation is reasonable for a weakly interacting system as long as the mode damping rates are orders of magnitude smaller than the oscillator frequencies. The SCBA scheme guarantees current conservation, i.e. $I_L = -I_R$ [26].

We study a linear four-atom gold wire under two different states of strain, as shown in Fig. 1, corresponding to electrode separations of $L = 12.22$ Å and $L = 12.68$ Å. The semi-infinite gold electrodes are modelled as perfect (100) surfaces in a 3×3 unit cell. We take the electrode temperature to be $T = 4.2$ K as in the experiments. Allowing the wire atoms to move we calculate the phonon modes and energies for each of the two structures. In the AO basis we determine the static Hamiltonian of the whole system as well as the e-ph couplings. These are then downfolded on the basis of the four wire atoms (which constitutes region C) with self-energies $\mathbf{\Sigma}_\alpha$ to represent the electrodes. We calculate the phonon signal in the non-linear differential conductance vs bias voltage ($G - V$) with Eq. (3) for two extremal cases: the energy transferred from the electrons to the vibrations is either (i) instantaneously absorbed into an external heat bath, or (ii) accumulated and only allowed to leak via electron-hole (e-h) pair excitations. We will refer to these limits as the externally damped and externally undamped cases, respectively.

The externally damped limit corresponds to each mode having a fixed occupation $N_\lambda \approx 0$ as set by a Bose-Einstein distribution with a temperature $T = 4.2$ K. This leads to the results shown in Fig. 2. The conductance is close to the quantum unit $G_0 = 2e^2/h$ for zero bias and

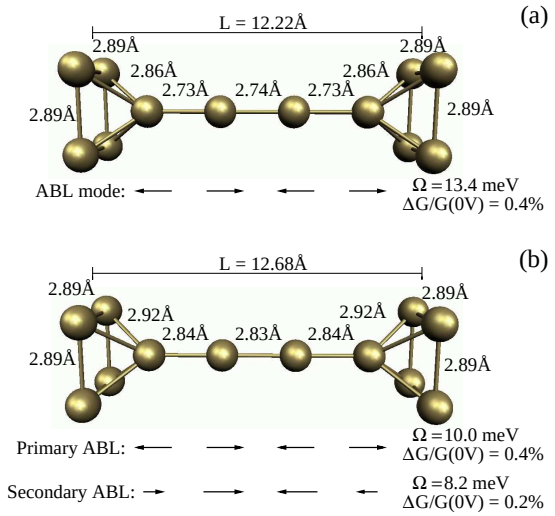

FIG. 1: Geometry of a four-atom gold wire under two different states of stress corresponding to an electrode separation of (a) $L = 12.22$ Å and (b) $L = 12.68$ Å. The electrodes are modelled as perfect (100) surfaces, from which only the atoms closest to the wire are shown. The ABL modes, which cause the inelastic scattering, are shown schematically with arrows below each structure, together with mode energy Ω_λ and extracted conductance drop $\Delta G/G(0\mathrm{V})$.

displays symmetric drops for finite bias. A comparison of the two structures indicates that straining the wire results in lower zero-bias conductance (related to weakened couplings to the electrodes) as well as mode softening and enhanced phonon signal. These three effects were also observed experimentally (the shift in zero-bias conductance being most dramatic close to rupture). The total conductance drops $\Delta G/G(V=0)$ are found to be 0.5% for the wire $L = 12.22$ Å and 0.7% for $L = 12.68$ Å. These drops occur at threshold voltages corresponding to the ABL mode energies. By including one mode at a time, we can investigate the contribution from each mode separately. This reveals that the inelastic scattering, for both geometries, originates only from longitudinal modes with ABL character. For the linear gold wire the conduction channels are rotationally invariant, hence they cannot couple to transverse modes. On the other hand for a zigzag conformation, which under certain strains is favorable [35], also transverse modes could possibly contribute. Indistinctness of such signals are thus fully compatible with a linear geometry. The importance of ABL character can be understood as a reminiscence of the momentum conservation in infinite one-dimensional wires, where the only allowed inelastic (intraband) transitions correspond to electrons interacting with phonons with a wavenumber of approximately twice the Fermi wavevector (backscattering) [11]. For $L = 12.22$ Å we find a conductance drop $\Delta G/G(V=0)$ from the ABL mode of 0.4%, and for $L = 12.68$ Å drops of 0.4% and 0.2% from the primary and secondary ABL mode, respectively. These modes and their contributions to the conductance are also shown in Fig. 1. The contribution from any other mode is found to be less than 0.06%.

The salient features of the experiments [10, 11], *viz.* (i) the order of magnitude of the conductance drop, (ii) the mode softening, and (iii) the increased phonon signal with strain, are all properly reproduced by our calculations. In particular, we find the same frequency shift with elongation ($\Delta\Omega/\Delta L = -7$ meV/Å) as observed experimentally. From our analysis we conclude that the enhanced signal with strain is not due to increased e-ph couplings, but rather due to the fact that the electronic structure changes. This change affects the bond strengths, and hence the normal modes of the structure, such that a second mode acquires ABL character. This is contrary to considerations based on an infinite one-dimensional wire model [11].

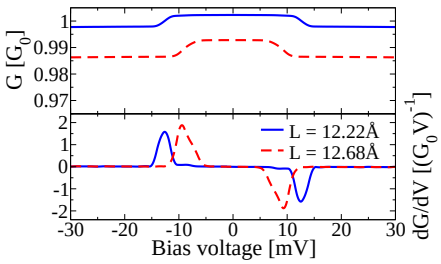

FIG. 2: Differential conductance and its derivative for the four-atom gold wire at two different tensions in the case where the oscillators are externally damped ($N_\lambda \approx 0$). All modes are included in this calculation.

In the externally undamped limit we determine the mode occupations for a given bias voltage using the fact that the system is in a steady state. With Eq. (4) we require that the net power into the device $P_L + P_R$, which equates the net power transferred from the electrons to the phonons, must be zero. This in turn puts a restriction on N_λ. For simplicity we include only the most important mode. The conductance calculation is shown in Fig. 3a. Compared with the externally damped results Fig. 2, the notable differences are a slightly larger drop as well as a finite slope in the conductance beyond the onset of inelastic scattering. Fig. 3b shows where the vibrational excitation sets in and starts to increase linearly with bias. At a voltage $V = 55$ mV the occupation is found to be the same as *if* the mode was occupied according to a Bose-Einstein distribution with temperature $T = 300$ K.

A finite slope was also observed in the experiments, and speculated to be directly related to nonequilibrium phonon populations [11]. This is confirmed by our calculations. Quantitatively we find $dG/dV(20\text{mV}) \approx -0.6\,(G_0\text{V})^{-1}$ and $dG/dV(20\text{mV}) \approx -0.7\,(G_0\text{V})^{-1}$ for $L = 12.22$ Å and $L = 12.68$ Å, respectively, which is only slightly larger than detected for relatively long gold wires. In reality the phonon modes are damped also by mechanical coupling to bulk phonons in the electrodes. This coupling depends strongly on the nature of the chain-electrode contact and hence, understood poorly. We expect that the typical damping conditions lead to $G - V$ curves in between Fig. 2 and Fig. 3a.

The observed linewidth of the phonon signal is set by a combination of both electronic temperature and mode broadening [8]. The temperature broadening alone is of

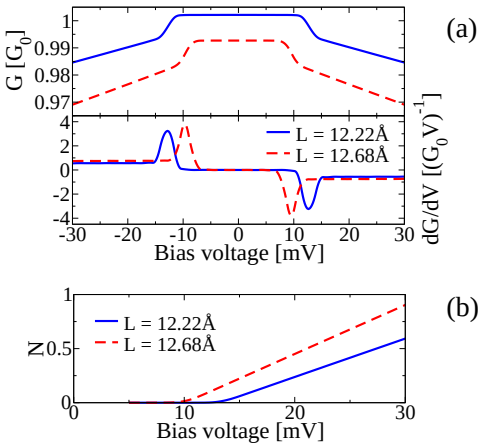

FIG. 3: (a) Differential conductance and its derivative for the four-atom gold wire at two different tensions in the externally undamped limit. Only the most important mode is included in this calculation. (b) Mode occupation N vs bias voltage.

the order $5k_BT \approx 2$ meV (FWHM). As the atomic wire is elongated, new modes contribute to the drop. Hence, our calculations show that the corresponding linewidth will increase from 2 to 4 meV due to the appearance of a second mode, cf. Fig. 2. In addition to this, mode broadening due to coupling to the electrons and to vibrations in the bulk also contribute. We estimate the damping of the modes from e-h pair generation to be no more than $\gamma_{\text{e-h}} = 30\text{-}35$ μeV [36], which is thus negligible here. In the experiment the linewidth is typically around 5 meV, and hence it is either a result of the overlap of several vibrational modes or due to significant coupling to bulk modes. This could be clarified with measurements at even lower temperatures, where it might be possible to resolve several modes as a function of the wire strain.

As we show elsewhere [26, 37], it is possible to describe the system qualitatively with a single-orbital tight-binding model. Using this simplified approach longer chains can be examined, for which first-principles calculations are not feasible at the present stage. The simple model predicts that the conductance drop $\Delta G/G(V = 0)$ and slope dG/dV beyond the threshold scale linearly with the number of atoms in the wire (we considered up to 40 atoms). This supports the notion that the inelastic scattering occurs inside the wire itself.

In conclusion, we investigated inelastic effects in atomic gold wires using a first-principles approach. We calculated the non-linear differential conductance for two structures of a four-atom wire, and clarified the mode selectivity observed experimentally as well as the mechanism behind phonon signal increase with elongation. Further, we considered two extremes of external mode damping, which lead to the suggestion that local "heating" of the wire is significant in the experiment.

We thank the French Embassy in Copenhagen for financial help and acknowledge stimulating discussions with M. Paulsson. M.B. thanks the CNRS for a "poste de chercheur associé," and N.L. is grateful to the ACI jeunes chercheurs. We also thank the Danish Center for Scientific Computing (DCSC), the Centre d'Informatique de l'Enseignement Supérieur (CINES), and the Centre de Calcul de Midi-Pyrénnées (CALMIP) for computational resources.

* Electronic address: thf@mic.dtu.dk

[1] N. Agraït, A. L. Yeyati, and J. M. van Ruitenbeek, Phys. Rep. **377**, 81 (2003).
[2] M. A. Reed *et al.*, Science **278**, 252 (1997).
[3] R. H. M. Smit *et al.*, Nature (London) **419**, 906 (2002).
[4] S. Kubatkin *et al.*, Nature (London) **425**, 698 (2003).
[5] J. G. Kushmerick *et al.*, Nano Lett. **4**, 639 (2004).
[6] W. Wang *et al.*, Nano Lett. **4**, 643 (2004).
[7] R. H. M. Smit, C. Untiedt, and J. M. van Ruitenbeek, Nanotechnology **15**, 472 (2004).
[8] P. Hansma, Phys. Rep. **30**, 145 (1977).
[9] B. C. Stripe, M. A. Rezaei, and W. Ho, Science **280**, 1732 (1998).
[10] N. Agraït *et al.*, Phys. Rev. Lett. **88**, 216803 (2002).
[11] N. Agraït *et al.*, Chem. Phys. **281**, 231 (2002).
[12] J. Lambe and R. C. Jaklevic, Phys. Rev. **165**, 821 (1968).
[13] J. Appelbaum and W. Brinkman, Phys. Rev. **186**, 464 (1969).
[14] C. Caroli *et al.*, J. Phys. C **5**, 21 (1972).
[15] J. Bonča and S. A. Trugman, Phys. Rev. Lett. **75**, 2566 (1995).
[16] E. G. Emberly and G. Kirczenow, Phys. Rev. B **61**, 5740 (2000).
[17] M. Brandbyge *et al.*, Phys. Rev. B **65**, 165401 (2002).
[18] N. Mingo and K. Makoshi, Phys. Rev. Lett. **84**, 3694 (2000).
[19] N. Lorente and M. Persson, Phys. Rev. Lett. **85**, 2997 (2000).
[20] M. J. Montgomery *et al.*, J. Phys. Condens. Matter **15**, 731 (2003).
[21] M. J. Montgomery and T. N. Todorov, J. Phys. Condens. Matter **15**, 8781 (2003).
[22] S. Alavi *et al.*, Chem. Phys. **281**, 293 (2001).
[23] Y.-C. Chen, M. Zwolak, and M. Di Ventra, cond-mat/0402536.
[24] H. Ness, S. A. Shevlin, and A. J. Fisher, Phys. Rev. B **63**, 125422 (2001).
[25] K. Flensberg, Phys. Rev. B **68**, 205323 (2003).
[26] T. Frederiksen, Master's thesis, Technical University of Denmark (2004).
[27] M. Galperin, M. A. Ratner, and A. Nitzan, cond-mat/0405343.
[28] J. P. Perdew, K. Burke, and M. Ernzerhof, Phys. Rev. Lett. **77**, 3865 (1996).
[29] In the PW calculations we use 3-atom-thick slabs for electrodes. The geometric and vibrational properties were determined by using the ultra-soft pseudopotential PW code DACAPO (`www.fysik.dtu.dk/campos/Dacapo`) converged with 25 Ry cutoff. The k-point sampling was particularly critical in determining the geometry and vibrational modes. The calculations were converged at a k-point sampling of $6 \times 6 \times 1$ and relaxation criterium until forces on wire-atoms were smaller than 0.03 eV/Å. The modes were calculated by diagonalizing the dynamical matrix evaluated by finite difference (0.03 Å).
[30] J. M. Soler *et al.*, J. Phys.: Condens. Matter **14**, 2745 (2002).
[31] We use TRANSIESTA with the same settings as in [17] and a single-ζ plus polarization basis set of nine orbitals corresponding to the $5d$ and $6(s, p)$ states of the free atom.
[32] M. Head-Gordon and J. C. Tully, J. Chem. Phys. **96**, 3939 (1992).
[33] H. Haug and A.-P. Jauho, *Quantum Kinetics in Transport and Optics of Semiconductors* (Springer, 1996).
[34] Y. Meir and N. S. Wingreen, Phys. Rev. Lett. **68**, 2512 (1992).
[35] D. Sánchez-Portal *et al.*, Phys. Rev. Lett. **83**, 3884 (1999).
[36] B. Hellsing and M. Persson, Phys. Scr. **29**, 360 (1984).
[37] T. Frederiksen *et al.*, cond-mat/0411108.